UNIVERSITY OF CAPE TOWN

FACULTY OF ENGINEERING

DEPARTMENT OF MECHANICAL ENGINEERING

CREEP PREDICTIONS FOR TURBOMACHINERY COMPONENTS

a dissertation submitted towards the degree of
Master of Science in Engineering

H. O. SIEBURG
B. Sc. Eng. (Mech.) (Witwatersrand)

April 1989

ABSTRACT

Several theories of creep and creep rupture are reviewed. Specific attention is devoted to the brittle damage theory proposed by Kachanov. Creep, damage and life predictions for rectangular or circular cross section beams under bending and tensile loads are presented. Comparison with data for a Ni Superalloy showed life predictions could be 30% in excess of experimental values. This beam model also revealed that it is imperative that no bending moments be inadvertently applied during tensile creep testing. The creep-damage material model is extended to multidimensional situations. A refinement, whereby no damage accumulates in compression, is incorporated. A User-Material subroutine for this constitutive model has been formulated, and incorporated into the ABAQUS FEM package. Several verification examples are presented; one example is the creep-damage behaviour of a notched bar in tension. The value of reference stress techniques is discussed. Reference stress estimates for a centrifugally loaded bar, as well as for a cantilever under distributed loads, are presented. These could be useful in turbine blade design.

ACKNOWLEDGEMENTS

Financial support from the FRD of the CSIR is gratefully acknowledged.

I would like to thank Mr. N.J. Marais from AMRU, UCT for assisting with the formulation of the User Material subroutine.

Lastly, my thanks to Prof. R.K. Penny for his guidance through the topic.

CONTENTS

PAGE

1.0 Introduction

At high temperatures, typically above 3/10 of the melting point, materials behave differently to the familiar elastic-plastic responses at room temperature: There is a continual, although slight, increase in deformation under load. Then after several hundred (or thousand) hours of apparently safe operation, the component fails catastrophically and without much prior warning. This creep phenomenon is not yet fully understood.

In many applications such as steam generators, furnaces, steam or gas turbines, creep has been observed to occur. The designers of such apparatus cannot predict with acceptable confidence what the time to failure under operating conditions is likely to be. Yet the prevention of a catastrophic failure is imperative.

Researchers and Engineers are continuously striving towards a better understanding of this creep phenomenon, so as to develop better analysis and design tools.

This work has been conducted in order to become familiar with contemporary thinking on this subject, and to become familiar with some of the creep analysis tools.

1.1 Scope of proposed work

Firstly the theories of creep deformation and damage were reviewed in order to assess those characteristics needed for the design of structures operating in the creep range. The finite lifetimes of creeping structures were of particular interest.

Reference stress techniques were studied. The technique is an approximate, but useful aid for component design in the creep range.

As an introduction to the topic, creep-damage in beams of various cross-sections, under bending and/or axial loads, were investigated.

To perform advanced calculations, non-linear finite element methods were used. The ABAQUS finite element package was used, as it provided the possibility for a user to define his own material constitutive relations. A subroutine UMAT, capable of portraying creep and damage behaviour, was developed and verified.

It was proposed that ultimately these relevant theories and finite element subroutines should be used in design calculations of creep damage of structures at high temperatures such as turbine blades and thin walled structures.

Non-isothermal and thermal transient conditions, although very pertinent to the creep problem, were not considered here.

2.0 Literature survey

2.1 Creep deformation under constant stress

When a specimen, maintained at a suitably high temperature, is subjected to constant uniaxial tension, a time dependent deformation over and above an elastic deformation is observed. Early investigators have tended to identify 4 distinct phases of the deformation response:

1) Immediate elastic deformation.

2) Primary creep, characterised by a decreasing strain rate.

3) Secondary creep, during which the strain rate is constant.

4) Tertiary creep, where the strain rate increases and finally the specimen parts, i.e. rupture.

illustrated in fig. (2.1) from [1]:

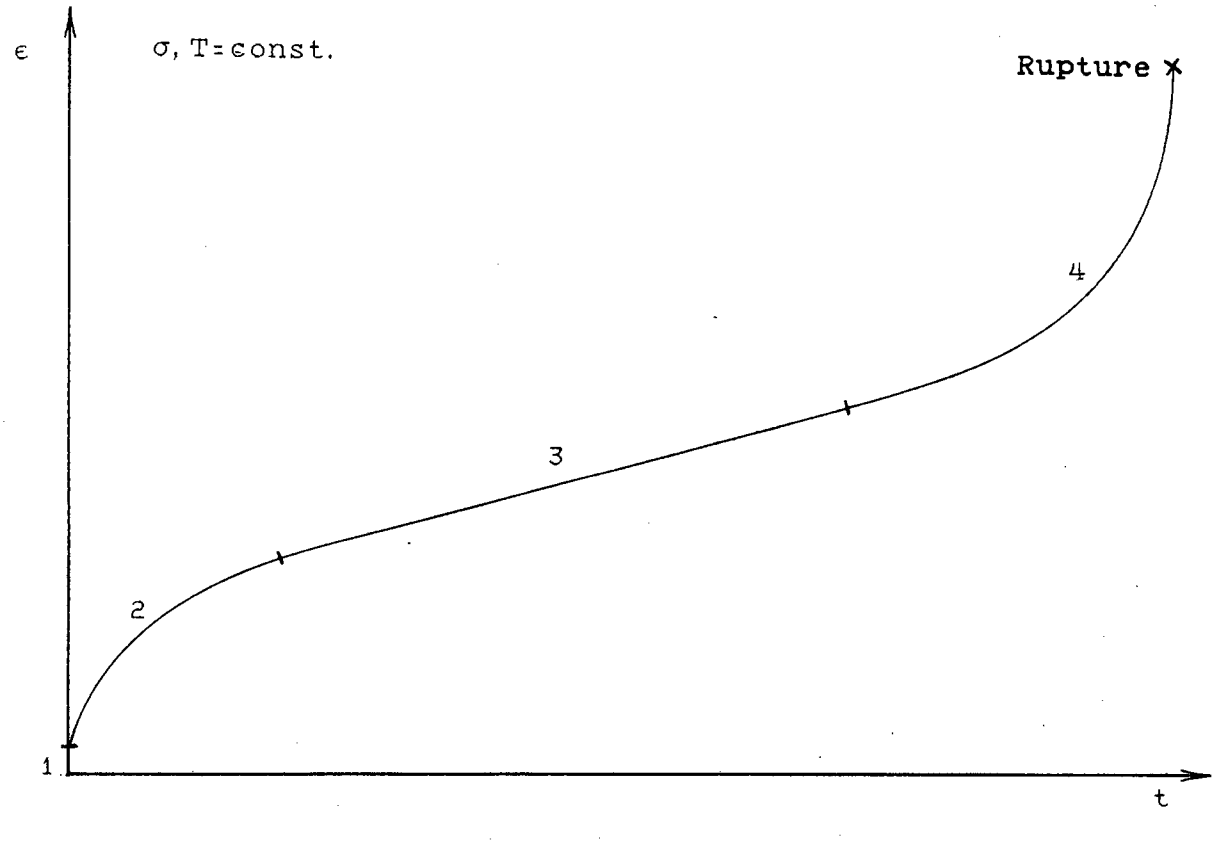

fig. (2.1) Creep response to a uniaxial load

It is claimed that different deformation mechanisims dominate during primary, secondary and tertiary creep phases.
Besides geometry and material properties, the deformation was found to be dependent on three major parameters: stress (σ), time (t) and temperature (T) [1], i.e.

$$\varepsilon_{cr} = f(\sigma, t, T)$$

The proposal that the variables can be separated is mathematically convenient and widely accepted, but is however not conclusively proven. So:

$$\epsilon_{cr} = f_1(\sigma)\ f_2(t)\ f_3(T)$$

Early investigators proposed many function types for f_1, f_2 and f_3 based on empirical considerations on rate processes. By curve-fitting procedures they described the creep phenomenon with some success. However a unifying empirical rationale remains elusive.

Norton (from [1]) proposed a power relationship for f_1 which yields good results for lower stresses:

$$f_1(\sigma) = A\ \sigma^m \qquad \ldots \quad (2.1)$$

Dorn [2] proposed an exponential relationship for f_1 which gives better results at higher stresses:

$$f_1(\sigma) = C\ \exp(\sigma/\sigma_o)$$

And Mc. Vetti [3] attempted to unify the above approaches by stating:

$$f_1(\sigma) = \sinh^m(\sigma/\sigma_o)$$

noting that a sinh function approaches a power function for lower stress values, and an exponential function at high stress values.

The Norton relationship is however most widely used.

Functions f_2 for the time dependence are variations of a power relation, for example:

$$f_2(t) = \alpha\ t^n \qquad 1/3 < n < 1/2 \qquad \ldots \quad (2.2)$$

attributed to Bailey [1]. Graham and Walles proposed:

$$f_2(t) = \sum_i \alpha_i t^{n_i}$$

and the specific form:

$$f_2(t) = \alpha t^{0.33} + \beta t + \gamma t^3$$

is frequently used [4] as it gives good results for many materials.

Temperature affects creep response in several ways. Firstly, the material properties are functions of temperature. So for f_1 and f_2 above:

$$A = A(T)\ , \quad m = m(T)\ , \quad \alpha = \alpha(T)\ , \quad n = n(T) \quad \text{etc.}$$

Secondly, different deformation and damage mechanisims dominate the creep response at increasing operating temperature. At lower temperatures dislocation mobility and consequent slip

within crystals predominate. At higher temperatures increased dislocation mobility and diffusion cause intercrystalline slip and void formation to dominate.

The general consensus appears to be that the effect of temperature should be described by the form:

$$f_3(T) = f_3\left[\exp\left[\frac{-Q}{RT}\right]\right]$$

where Q = activation energy and R = Bolzmann constant. Power functions for f_3 are generally used. There is significant evidence, however, to suggest that functions for the time and temperature variables must not be separated, but should be treated as some time-temperature parameter. Dorn proposed a power function [2]:

$$f_{2,3} = \alpha\left[t\,\exp\left[\frac{-Q}{RT}\right]\right]^n$$

Time-temperature relationships have been used successfully to extrapolate rupture data using the Larson-Miller or Manson-Halferd parameters for instance [5]. The relative success in using such parameters is evidence that time and temperature must be seen in conjunction.
A more complete list of possible functions can be found in [6].

2.2 Creep under variable stresses

A multitude of theories have been proposed, many of which are significant and useful, however no one single theory is acceptable for all conditions. As before only the more widely used theories will be described [1].

2.2.1 Time hardening

is based on the assumption that the major factor affecting the creep rate is the length of exposure to a temperature and stress level, irrespective of the strain history [5]. It asserts therefore that only material changes are significant. If f_1 and f_2 are chosen as eq. (2.1) and (2.2) respectively, and for constant temperature:

$$\dot{\epsilon}_{cr} = nA\ \sigma^m\ t^{n-1} \qquad \ldots \quad (2.3)$$

A graphic procedure is summarised in fig. (2.2) from [5].

2.2.2 Strain hardening

is based on the assumption the the major factor affecting the creep rate is the state of strain, irrespective of its exposure time [5]. So it is claimed that an equation of state governs the creep response. If eq. (2.1) and (2.2) are chosen as before, and given constant temperature:

$$\dot{\epsilon}_{cr} = \frac{nA^{1/n}\ \sigma^{m/n}}{\epsilon_{cr}^{(1-n)/n}} \qquad \ldots \quad (2.4)$$

Strain hardening is illustrated graphically in fig. (2.3) from [5].

2.2.3 Life fraction rule (Robinson)

This refinement attempts to compromise between time hardening and strain hardening. Instead of moving vertically (fig. 2.2) or horisontally (fig. 2.3) to determine the starting point on the new curve, an intermediate starting point is chosen so that the ratios of exposure time to rupture-life on the curve and a subsequent curve are equal, i.e.:

$$\frac{t_i}{t_{Ri}} = \frac{t_f}{t_{Rf}} \qquad t_f = \frac{t_{Ri}}{t_{Rf}}\ t_i$$

t_f thus determines the starting point on a curve for the following stress level. The procedure is illustrated in fig. (2.4) from [5].

A close relationship can be shown to exist [1] between Kachanov damage accumulation and Robinsons Life Fraction rule.

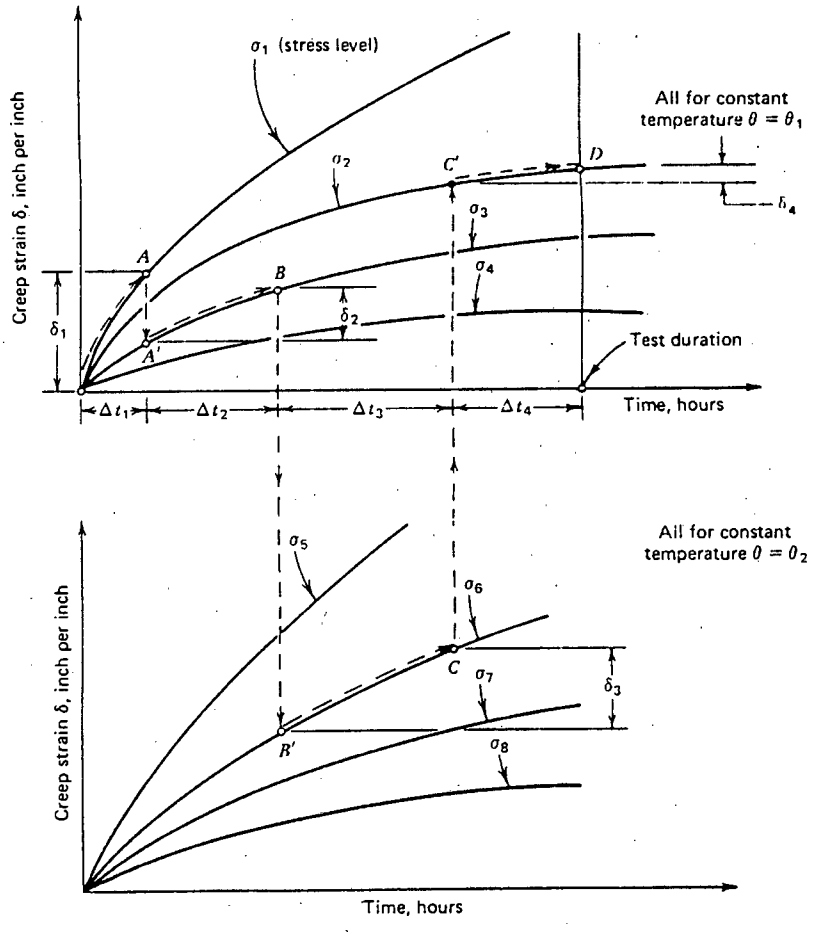

fig. (2.2) Creep strain accumulation under time-hardening assumptions

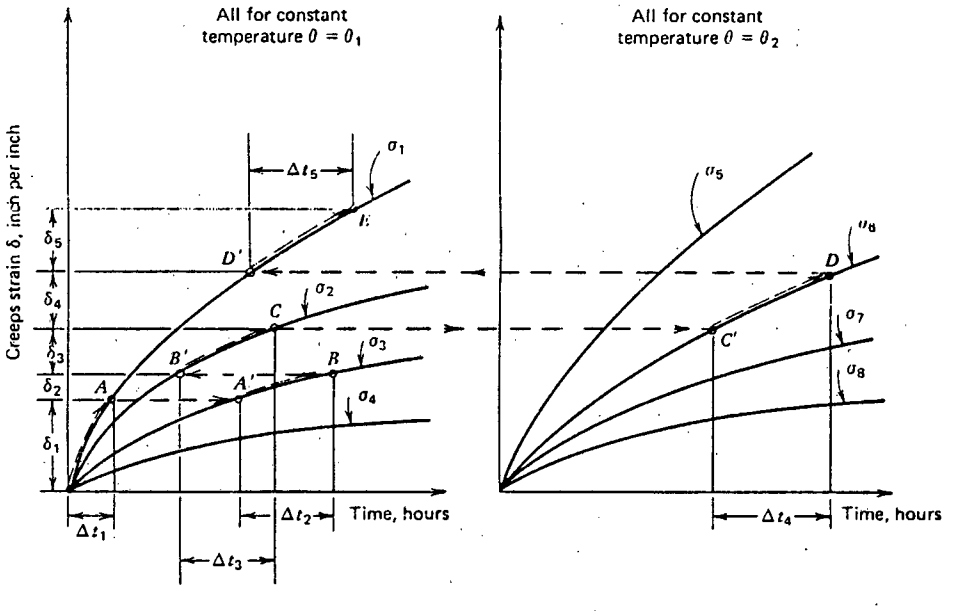

fig. (2.3) Creep strain accumulation under strain-hardening assumptions

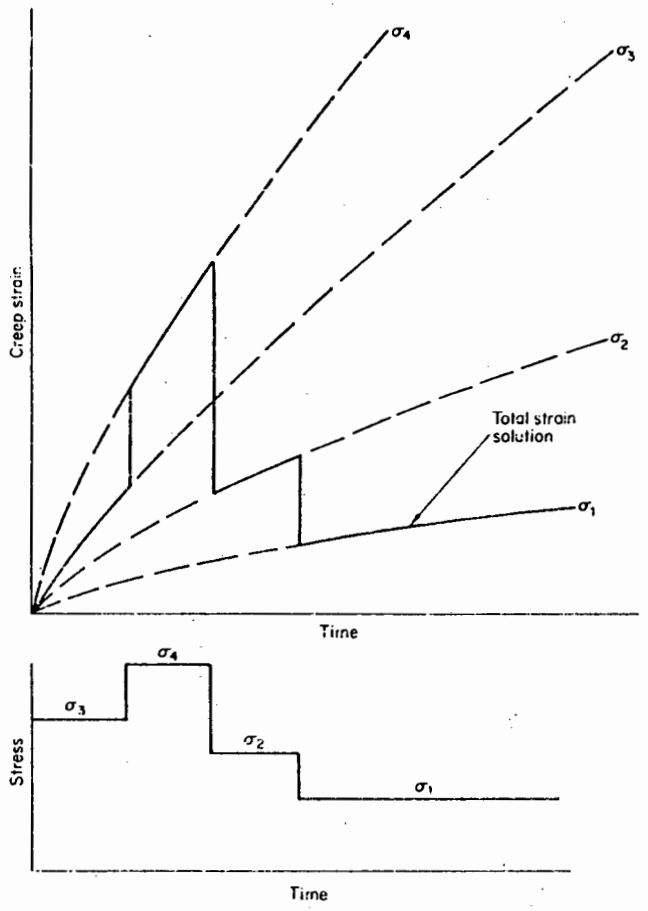

fig. (2.5) Creep strain accumulation under a total strain theory

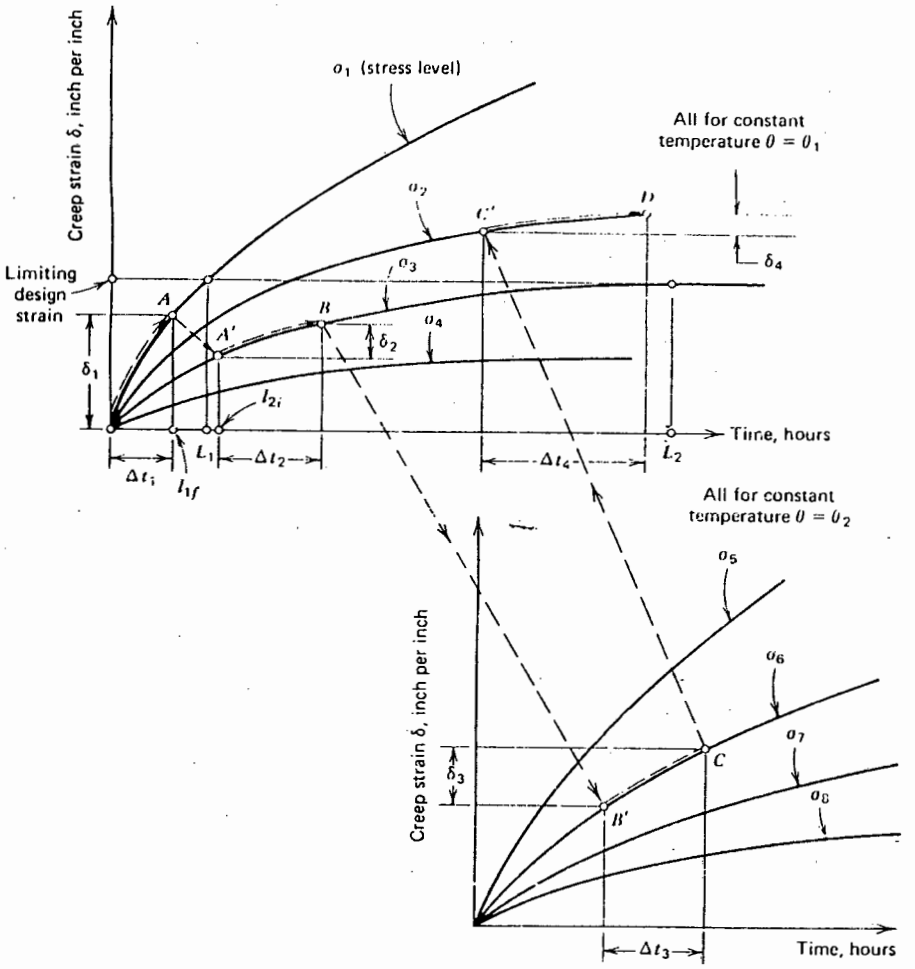

fig. (2.4) Creep strain accumulation under a life-fraction rule

2.2.4 Total strain theory

proposes that a one to one relationship between strain and time exists, even for variable stress. There is an immediate and complete response to stress changes. The theory is included, despite its inaccuracy, for its simple application and demonstrated in fig. (2.5) from [1].

The above theories can be compared by examining how each predicts primary creep response to a step load, as shown in fig(2.6):

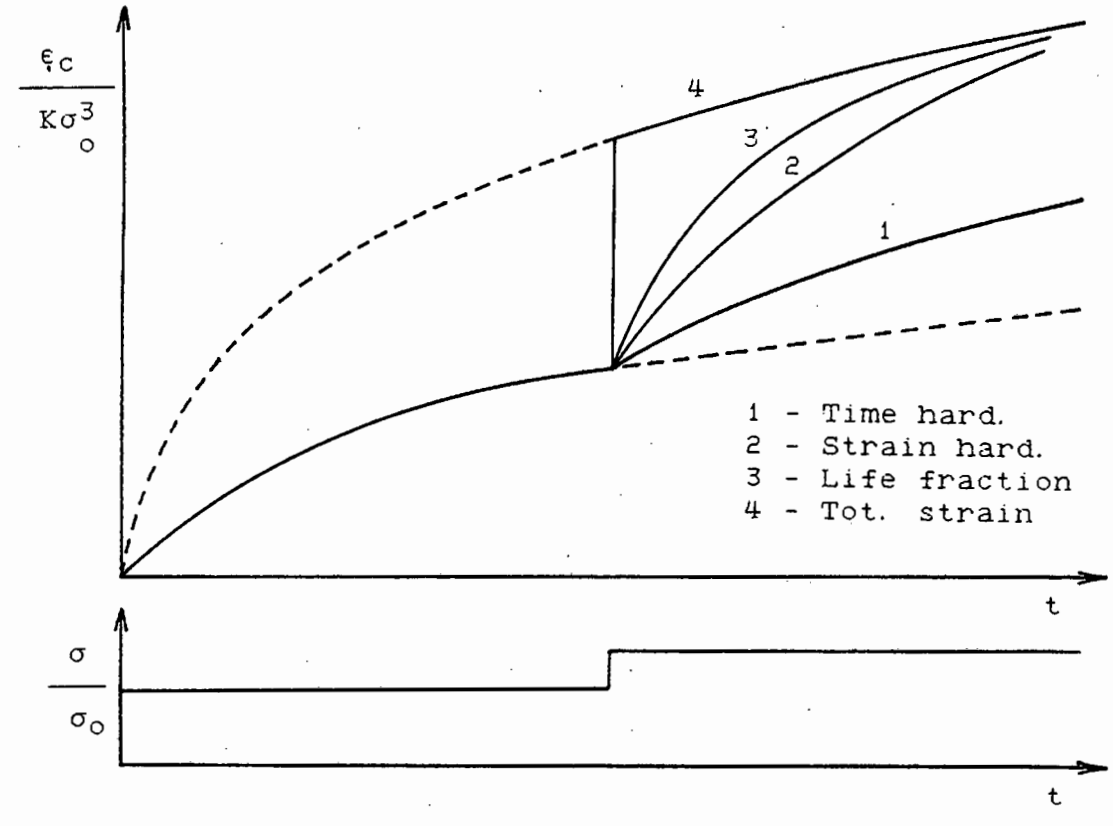

fig. (2.6) Response to a step load change

The predictions vary widely. With the exeption of the time hardening theory, all theories approach the total strain solution with time. The strain hardening theory correlates best with experimental data, and so would be the best theory to use. Time hardening and total strain theories, despite their inaccuracies, could serve to set upper and lower limits to creep curves. The real behaviour would lie between the time hardening and total strain extremes, and strain hardening would give a fair indication of the response.

2.2.5 Viscoelastic models

Attempts have been made to describe creep in terms of linear or nonlinear visco-elasticity, i.e. as an analogy to the behaviour of linear elasticity and viscosity of Newtonian fluids [7]. The approach is particularly useful when analysing variable loads [8].

Maxwell's model considers equilibrium of a spring and dashpot in series:

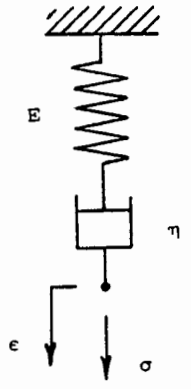

$$\sigma = E\epsilon + \eta\dot{\epsilon} \quad \text{ie.} \quad \sigma + p_1\dot{\sigma} = q_1\dot{\epsilon} \qquad p_1 = \eta/E \;,\; q_1 = \eta$$

and using Laplace transforms the response to any loading function can be obtained:

$$\epsilon(t) = \int_0^t \sigma(\tau)\left[1/\eta + 1/E\ \delta(t-\tau)\right]\partial\tau$$

Although primary and tertiary creep are not reproduced, the model does qualitatively reproduce the interaction of secondary creep with elastic deformation as shown in fig. (2.7) for a step load.

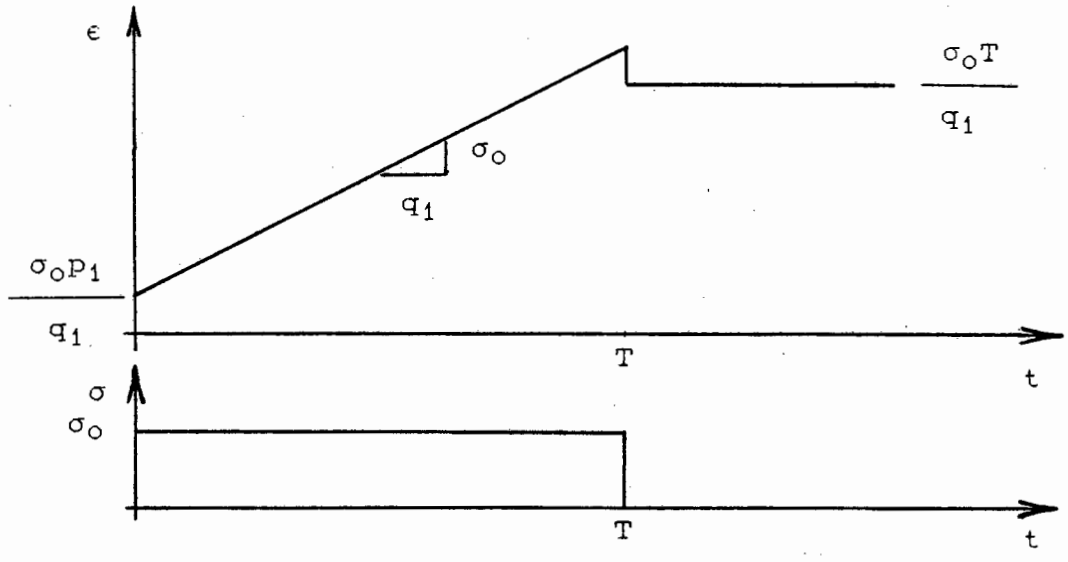

fig. (2.7) Response to step load changes

A Kelvin solid considers a spring and dashpot in parallel, and by a similar analysis obtains the response to any loading function to be:

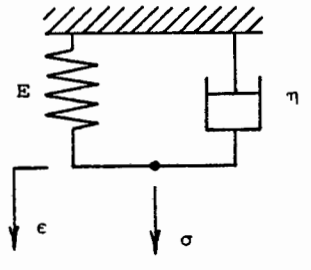

$$\epsilon(t) = 1/\eta\int_0^t \sigma(\tau)\ \exp\left[E/\eta(\tau-t)\right]\ \partial\tau$$

Only primary creep and recovery is reproduced as illustrated in fig. (2.8) for a step load:

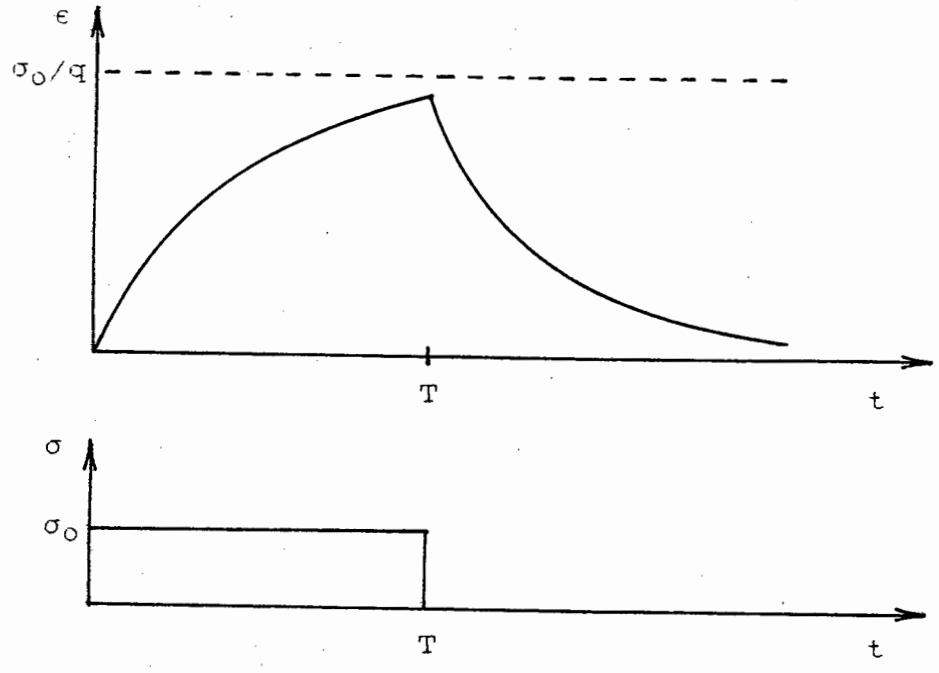

fig. (2.8) Response to step load changes

A Standard viscous solid is modelled by superimposing a Maxwell fluid and a Kelvin solid, and the response to any load function is:

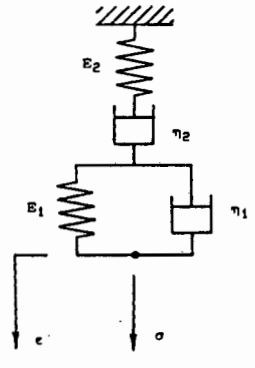

$$\epsilon(t) = 1/\eta_1 \int_0^t \sigma(\tau)\, \exp\left[(\tau-t)/m\right]\, \partial\tau + \int_0^t \sigma(\tau)\left[1/\eta_2 + 1/E_2\,\delta(t-\tau)\right]\, \partial\tau$$

With the exeption of tertiary creep all deformation phenomena can be described. Elastic deformation for loading and unloading are correctly modelled, and primary creep (modelled as a transient) asymptotically approaches secondary creep. This is illustrated in fig. (2.9):

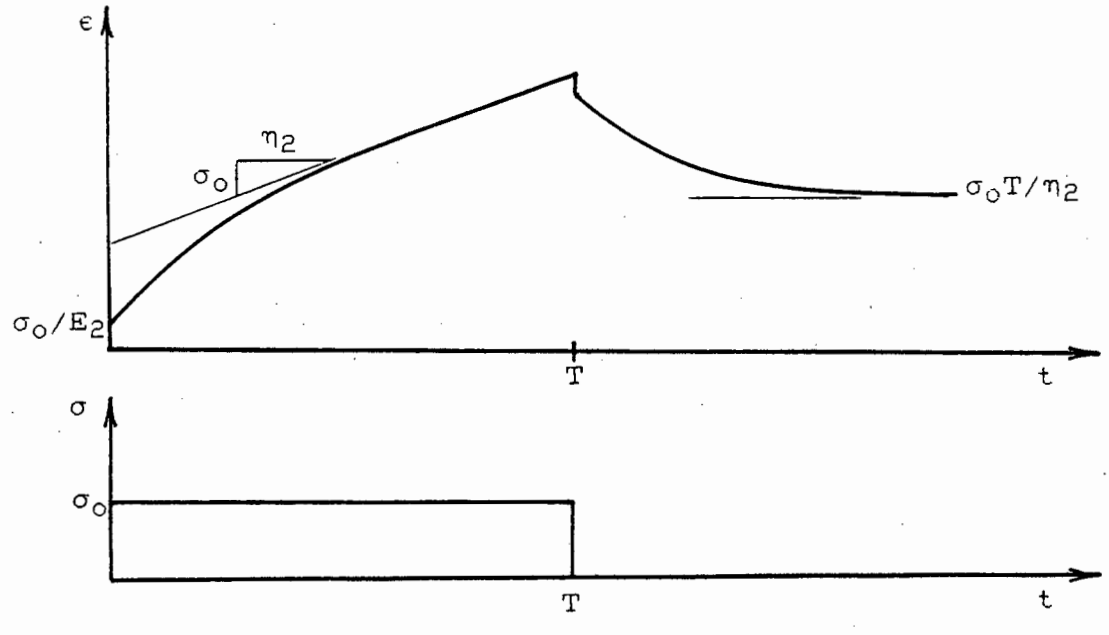

fig. (2.9) Response to step load changes

Although such an approach has been successful in describing the response of non-metals, it was found to be inappropriate when analysing creep behaviour of metals. Metallic creep is not only a viscous process, but rather diffusion and void formation are the dominant phenomena. However, purely qualitatively, primary and secondary creep are described using this approach.

Extensions to the above visco-elastic theories have been attempted:

1) By including more spring and dashpot elements in various arrangements, higher derivatives of stress and strain are introduced to the differential equation of equilibrium and solved. So for example, Besseling used several Maxwell-elements in parallel with some success.

2) By introducing non-linearities, i.e. terms p_i and q_i as variables of stress and temperature, very good theories were developed by Graham and Walles as well as Rabotnov (reviewed in [1]). These yield better correlation with experiment.

3) Gittus [9] has attempted to relate viscous terms in the differential equation of equilibrium to crystal dislocation processes and void formation.

2.3 Multiaxial creep

The largest proportion of creep tests are uniaxial tension tests. However realistic service applications involve multiaxial stresses. The uniaxial constitutive equations can readily be extended into the multiaxial domain.

Investigators have seen remarkable similarities between the creep process and plasticity. Both could be described as path dependent viscous flow. The similarity in stress distributions, once a steady-state is attained, supports the connection. The resulting model should comply with several requirements [1, 25]:

1) The multiaxial flow rule should reduce to the familiar uniaxial formulations when applied to a uniaxial tension test.

2) The model should reflect the observations that the material volume is (nearly) constant, and that the hydrostatic stress does not materially influence the creep process.

3) For isotropic materials, the principal stress and strain rate directions should coincide.

From 2), the creep strain rate is proportional to the stress deviator s_{ij}:

$$\frac{\partial \epsilon_{crij}}{\partial t} = \lambda \, s_{ij} \qquad \ldots \quad (2.5)$$

λ being a proportionality constant. This flow rule is an extension of the incremental Prandtl-Reuss plasticity flow rule to the creep regime.

Let the effective (v. Mises) stress and effective creep strain rate be:

$$\sigma_e = \frac{1}{\sqrt{2}}\left[(\sigma_{11}-\sigma_{22})^2+(\sigma_{22}-\sigma_{33})^2+(\sigma_{33}-\sigma_{11})^2+6\sigma_{12}^2+6\sigma_{23}^2+6\sigma_{31}^2\right]^{1/2} \qquad \ldots \quad (2.6a)$$

$$\frac{\partial \epsilon_{cre}}{\partial t} = \frac{\sqrt{2}}{3}\left[\left[\frac{\partial \epsilon_{11}}{\partial t}-\frac{\partial \epsilon_{22}}{\partial t}\right]^2+\left[\frac{\partial \epsilon_{22}}{\partial t}-\frac{\partial \epsilon_{33}}{\partial t}\right]^2+\left[\frac{\partial \epsilon_{33}}{\partial t}-\frac{\partial \epsilon_{11}}{\partial t}\right]^2+ 6\left[\frac{\partial \epsilon_{12}}{\partial t}\right]^2+6\left[\frac{\partial \epsilon_{23}}{\partial t}\right]^2+6\left[\frac{\partial \epsilon_{31}}{\partial t}\right]^2\right]^{1/2}_{cr} \qquad \ldots \quad (2.6b)$$

then:

$$\frac{\partial \epsilon_{crij}}{\partial t} = \frac{3}{2}\,\frac{\partial \epsilon_{cre}}{\partial t}\,\frac{s_{ij}}{\sigma_e} \qquad \ldots \quad (2.7)$$

The proportionality constant λ can be experimentally obtained from a uniaxial tension test, where the effective stress and strain reduce to the axial stress and strain respectively. Alternatively, a constitutive model and hardening hypothesis from chapter 2.2 can be used. So in general:

$$\epsilon_{cre} = f_1(\sigma_e)\ f_2(t)\ f_3(T)$$

Using the Norton and Bailey relationships under isothermal conditions (ie f_3=const.):

$$\epsilon_{cre} = a\sigma_e^{m}\ t^{n}$$

yields [25]:

$$\frac{\partial \epsilon_{crij}}{\partial t} = \frac{3}{2}\, an\sigma_e^{m-1}\, s_{ij}\, t^{n-1} \qquad \ldots \quad (2.8a)$$

for time-hardening, and

$$\frac{\partial ecrij}{\partial t} = \frac{3}{2}\, na^{1/n}\, \sigma_e^{(m/n-1)} s_{ij}\, \epsilon_{cre}^{(1-1/n)} \qquad \ldots \quad (2.8b)$$

for strain-hardening assumptions. The effect of damage can be incorporated by noting that:

$$\sigma_e = \frac{\sigma_{eN}}{1-\omega} \qquad \text{and} \qquad s_{ij} = \frac{s_{ijN}}{1-\omega}$$

The subscript N refers to stresses in the undamaged state.

In order to cast the time-hardening constitutive equations into a more useful (integrable) form, Penny [1] utilised the time transformation:

$$\tau = \int_0^t aE\ \sigma_o^{m-1}\ f_2(t)\ dt \quad = at^n$$

together with the normalisation of stress and strain quantities with respect to their corresponding reference stress and strain. If the non-dimensional quantities:

$$\Sigma_{ij}=\frac{\sigma_{ij}}{\sigma_o} \quad \Sigma_{ijN}=\frac{\sigma_{ijN}}{\sigma_o} \quad \Sigma_e=\frac{\sigma_e}{\sigma_o} \quad \Sigma_{eN}=\frac{\sigma_{eN}}{\sigma_o} \quad D_{ij}=\frac{s_{ij}}{\sigma_o} \quad D_{ijN}=\frac{s_{ijN}}{\sigma_o}$$

$$\lambda_{ij}=\frac{\epsilon_{ij}}{\epsilon_o} \qquad \lambda_e=\frac{\epsilon_e}{\epsilon_o} \qquad \lambda_{crij}=\frac{\epsilon_{crij}}{\epsilon_o}$$

are used, then the time transformation yields:

$$\dot{\lambda}_{crij} = \frac{3}{2}\, \frac{\dot{\lambda}_{cre}}{\Sigma_e}\, D_{ij} \qquad \text{with} \quad \dot{(\ )} = \frac{\partial(\ )}{\partial \tau}$$

and:

$$\dot{\lambda}_{cre} = \Sigma_e^m$$

Incorporating damage effects, the final creep constitutive equation is:

$$\dot{\lambda}_{crij} = \frac{3}{2} \frac{\Sigma_{eN}^{m-1} D_{ijN}}{(1-\omega)^m} \quad \ldots \quad (2.9)$$

If the refined damage model is used, whereby damage and damage accumulation is supressed in compression, equation (2.9) becomes:

$$\dot{\lambda}_{crij} = 3/2 \; \Sigma_{Ne}^{m-1} S_{Nij} \qquad \Sigma_1 < 0 \quad \ldots \quad (2.9a)$$

whenever the maximum principal stress is compressive.

2.4 Damage and creep rupture

Creep rupture is the culmination of the tertiary stage of creep, where the creep rate increases from a constant value (at the onset of tertiary creep) to infinity at rupture. Depending on stress and temperature, different microstructural processes dominate deformation behaviour, resulting in either a ductile or brittle fracture [1].

For temperatures above 0.4-0.6 of the melting temperature, failure is predominantly brittle. At such high temperatures diffusion becomes significant. Diffusion, coupled with increased dislocation mobility, results in the grain-boundaries becoming weaker than the grains themselves. Thus deformation occurs by slip along grain-boundaries. Also, prior to tertiary creep, there is little deformation. To maintain material continuity, the grains will deform. However, given suitable grain geometries and grain boundary slippage [1], the weaker grain boundaries separate, creating voids.

Metallographic investigations reveal that as tertiary creep begins, internal micro-voids do occur at grain boundaries. The voids are distributed throughout the material, but especially in high stress regions. It was shown that voids preferentially grow on a plane normal to the direction of maximum principal stress. Voids grow and coalesce to eventually form a macroscopic crack which at rupture has grown to a critical size [13].

For lower temperatures and higher stresses, different mechanisims predominate, causing ductile behaviour [14]. Due to lower temperatures, diffusion is markedly reduced. Slip occurs largely within the grains due to dislocation movement, but is restricted by the stable grain boundaries. Slip occurs preferentially along planes parallel to the maximum shear stress, so large strains and necking are observed. Excessive slip along a slip plane will cause cracks to be initiated at the surface [1]. Unlike brittle behaviour, cracks are not evenly distributed. There are only a few, ultimately only one dominant crack which grows along a slip plane.

The majority of creep tests are conducted under isothermal conditions to establish a relationship between rupture time and a constant uniaxial stress, shown in fig. (2.10).

The high stress, short time portion of the curve can be correlated to predominantly ductile behaviour. The low stress, long time part of the curve describes predominantly brittle behaviour. Both ductile and brittle rupture can be approximated by straight lines. A significant transition region shows that brittle and ductile mechanisims interact. So only when low stresses prevail, resulting in very long lifetimes, can ductile behaviour be safely neglected, and only when the stresses are very high can brittle void formation be safely ignored. As finite life at zero load is unreasonable, one would expect the rupture curve to asymptotically approach $t=\infty$ for extremely low stresses.

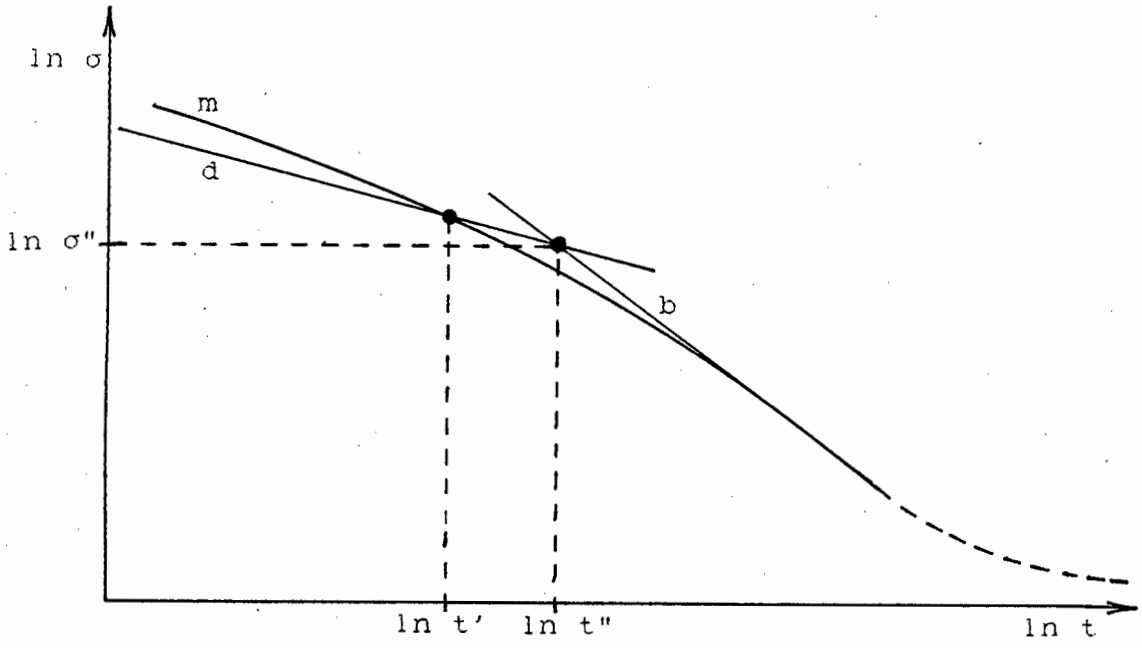

fig. (2.10) Time to rupture in uniaxial tension

The above description is a gross simplification of real behaviour, as oxidation, corrosion effects, phase transformations of crystal structure and recrystallisation contribute, and under certain circumstances even dominate, final response.

Until the complex creep process is more fully understood and described, a designer can only resort to phenomenological theories. One such theory, which appears especially promising, was proposed by Kachanov.

2.4.1 Kachanov brittle damage theory

Kachanov [14, 15] proposed that the observed growth and coalescence of microcracks can be described in terms of damage accumulation, irrespective of the mechanisim whereby they grow. So damage is defined as the progressive reduction of the cross section area of the material that bears load [25]. If $A(0)=A_N$ is the area of the undamaged component, then:

$$A(t) = A(0)\left[1-\omega(t)\right] \quad \text{i.e.} \quad A = A_N(1-\omega) \qquad 0 \leq \omega \leq 1$$

$\omega=0$ corresponds to virgin material containing no microcracks, and $\omega=1$ indicates complete seperation, i.e. rupture. Specifically, $\omega=1$ indicates the presence of a macroscopic crack of critical dimensions, whereupon rupture follows immediately. The requirement $\omega=1$ is thus the Kachanov criterion for rupture. Under constant loads, the stress will increase due to a reduction in area, so:

$$\sigma = \frac{\sigma_N}{(1-\omega)}$$

$\sigma_N = F/A_N$ being the stress in the undamaged component. Realising that damage accumulation is primarily dependent on stress, time, and temperature,

$$\omega = F_1(\sigma)\ f_2(t)\ F_3(T)$$

Kachanov proposed a power relationship for the stress dependence, similar to Norton's law for creep. So under isothermal conditions (F_3=const.):

$$\omega = b\ \sigma^k\ t^n$$

so that

$$\frac{\partial \omega}{\partial t} = b\ \sigma^k\ n t^{n-1} \approx b\left[\frac{\sigma_N}{1-\omega}\right]^k \quad . \ . \ . \quad (2.10)$$

The exponent n does in practice not differ greatly from 1.0, so the explicit time dependence is often neglected. Rabotnov [14] generalised the above to obtain:

$$\frac{\partial \omega}{\partial t} = b\ \frac{\sigma_N^k}{(1-\omega)^r} \quad \text{and} \quad \frac{\partial \epsilon_{cr}}{\partial t} = a\ \frac{\sigma_N^m}{(1-\omega)^q}$$

However, the simplifying assumptions whereby m=q and k=r are acceptable considering scatter in experimental data. It was also found that for a wide range of materials, $k \approx 0.75\ m$ [15].

If we consider the stresses to have attained a steady-state, (σ=const.) the Kachanov and Norton equations above can in turn be integrated w.r.t. time:

$$\int_0^1 (1-\omega)^k\ d\omega = b\sigma_N^{\,k} n \int_0^{t_R} t^{n-1}\ dt$$

if ω=1 the time to brittle rupture is:

$$t_R^{\,n} = \frac{1}{b(k+1)\sigma_N^k} \quad . \ . \ . \quad (2.11)$$

so

$$(1-\omega)^{k+1} = 1 - \frac{t}{t_R}$$

These results correlate well with experiment. Eq. (2.11) is plotted in fig. (2.10) as line b, and ductile fracture shown as line d. Substituting back into the Norton equation for creep strain and integrating we get:

$$\epsilon_{cr} = a\sigma_N^m t_R L\left[1-\left[1 - \frac{t}{t_R}\right]^{1/L}\right] \quad \text{with} \quad L=\frac{k+1}{k+1-m} \quad . \ . \ . \quad (2.12)$$

Upon rupture, when $t=t_R$ and $\epsilon_{cr}=\epsilon_R$:

$$\epsilon_{crR} = a\sigma_N^m t_R L = L/(k+1)\ a/b\ \sigma_N^{m-k}$$

The new material property L is the creep ductility. It measures the ability of the material to accommodate damage by redistributing stresses more evenly throughout the component [28].

The constants a and m can be obtained from short time creep tests. For many materials m=3 yields good results. If k≈3/4 m, the constants b and k can be obtained from rupture data and eq. (2.11) [15]. However eq. (2.11) is very sensitive to error, and rupture data is known to scatter considerably. So subsequent creep predictions will vary greatly for even small differences in b. Having obtained values for the constants from the limited data that is usually availible, creep curves can be constructed. Rupture times so predicted could, due to the extreme sensitivity mentioned, be 20-50 % in error.

A strain criterion for rupture ("e" criterion [1]) involves the Monkman-Grant constant ϵ_*. The criterion states simply that the minimum creep rate multiplied by the rupture time is a constant, a material property [19]. Noting that $a\sigma_N^m$ is the minimum creep rate, i.e. the steady-state creep rate which neglects damage-accumulation,

$$\epsilon_* = a\sigma_N^m \, t_R$$

This criterion can also be applied to obtain a further estimate for a.

As mentioned, the above analysis presumes constant stress; that the stress redistribution is complete. However, damage also accumulates during primary creep, where stresses redistribute. Also, the damage accumulation itself causes stresses to redistribute to maintain overall component equilibrium. It is thus questionable if a steady-state as such exists, although there are phases during the creep process where stresses vary only slightly with time (=secondary creep). In section 2.5, the numerical integration of the constitutive equations subject to varying stresses will be presented.

Multiaxial damage evolution involves the observation that for some materials the rupture life (and thus the damage accumulation) is governed by the maximum principal stress σ_1, whereas for other materials the effective (v.Mises) stress σ_e is more appropriate. Hayhurst [29] suggested that the shape of the isochronous rupture surface is:

$$\alpha \frac{\sigma_1}{\sigma_o} + (1-\alpha)\frac{\sigma_e}{\sigma_o} = 1.0$$

where the rupture time t_o is the life of a uniaxial tension test at the reference stress σ_o. The parameter α is a material constant. Kachanov's power relationship can now be extended to the multiaxial case:

$$\omega = b\left[\alpha\sigma_1 + (1-\alpha)\sigma_e\right]^k t^n$$

Utilising the same t-τ time transformation and non-dimensional quantities as in section 2.3, the multiaxial damage evolution equation is:

$$\dot{\omega} = \frac{b\sigma_o^{k+1-m}}{aE} \frac{\left[\alpha\Sigma_{1N} + (1-\alpha)\Sigma_{eN}\right]^k}{(1-\omega)^p} \qquad \ldots (2.13)$$

A further refinement in the damage evolution equation can be incorporated [18], to model void closure. It is argued that whenever the maximum principal stress is compressive, voids close. So in compression the entire (undamaged) cross-section area A_N becomes available to transmit loads. Thus

$$\omega=0 \ , \ \dot{\omega}=0 \text{ and } \sigma_{ij}=\sigma_{Nij} \qquad \text{if } \sigma_{N1}<0$$

The observation [18] that for comparable load magnitudes, the creep rupture times in compression are orders of magnitude higher than in tension, substantiates the model refinement.

2.4.2 Viscous failure (Hoff)

Given high loads and moderate temperatures, ductile materials will behave in a viscous manner [16]. Microvoids are less prevalant. The stress is increased by the Poisson effect reducing the cross sectional area. At a point of weakness, localised necking will occur, resulting in rupture. As the total strains are high, elastic strains may be neglected, but true stress and strain expressions must be used [14]. Here, only the uniaxial case will be discussed.

Differentiating the true stress-strain relationship, and substituting:

$$\dot{\epsilon}_{cr} = a\sigma^m \qquad \text{yields:} \qquad a\sigma^{m+1} = \dot{\sigma}$$

which can be integrated to obtain an estimate of the time to rupture:

$$t_R = \frac{1}{am\sigma_o^m}\left[1 - \left[\frac{\sigma_o}{\sigma_R}\right]^m\right] \qquad \ldots (2.14)$$

where σ_R is the stress when a localised neck occurs, and subsequent deformation is unstable to fracture. Rosenblyum [14] considered an elastic - perfectly plastic response by setting $\sigma_R=\sigma_y$, the yield stress at that operating temperature. For very very ductile materials, (especially pure materials) necking is extenive, and σ_R=infinity. Then the Hoff rupture life is:

$$t_R = \frac{1}{am\sigma_o^m} \qquad \ldots (2.15)$$

These times to ductile rupture are plotted in fig. (2.10) as line d. Brittle fracture is also shown as line b in fig. (2.10), so delineating the regions for brittle and ductile failure.

The intersection of the two curves b and d is at:

$$t'' = \frac{1}{am}\left[\frac{am}{b(k+1)}\right]^{-m/(m-k)} \qquad \text{and} \qquad \sigma'' = \left[\frac{b(k+1)}{am}\right]^{1/(m-k)}$$

This gives a rough indication that if $t>t''$ or $\sigma<\sigma''$ brittle fracture is likely, and if $t<t''$ or $\sigma>\sigma''$ ductile fracture is indicated.

Under variable loads, the Hoff ductile rupture equations also reduce to the familiar Robinsons Life Fraction rule.

For a work-hardening material with α the strain hardening exponent the Life Fraction rule in continuous form is:

$$\int_0^{\infty}\left[\frac{\epsilon_{cr}}{\epsilon_o}\right]^{\alpha}\exp(-m\epsilon_{cr})\,d\epsilon_{cr} = \int_0^{t} a\sigma_o^{m}\,dt = 1/m'$$

then:

$$t_R = \frac{1}{am'\sigma_o^{m}}$$

Besides integrating, m'is best obtained by experiment. It was found, however, that m'is not significantly different from m. Robinsons Life Fraction rule also applies to a work hardening material.

2.4.3 Kachanov mixed failure

Kachanov's brittle failure theory can be extended [14] by using true stress and strain when deformations are large. It is an attempt to extend the damage concept ω to the region of viscous failure. This can be done by noting that ω is defined as the reduction of cross-section area, by whatever mechanisim (ductile or brittle) it occurs. Kachanov proposed damage accumulation and creep progress independently, as they describe entirely different processes:

$$\dot{\epsilon}_{cr} = a\sigma_o^{m}\exp m\epsilon_{cr} \qquad \sigma = \left[\frac{\sigma_o}{1-\omega}\right]\exp(\epsilon_{cr})$$

and integrating:

$$\exp(\epsilon_{cr}) = \left[1 - am\sigma_o^{m}t\right]^{-1/m}$$

Kachanov proposed that damage accumulates according to:

$$\frac{\partial\omega}{\partial t} = b\sigma^{k} = b\left[\frac{\sigma_o}{1-\omega}\right]^{k}\exp(k\epsilon_{cr})$$

substituting for strain:

$$\frac{\partial\omega}{\partial t} = b\left[\frac{\sigma_o}{1-\omega}\right]^{k}(1-am\sigma_o^{m}t)^{-k/m}$$

Integrating over the lifetime, the rupture life predicted by the mixed Kachanov hypothesis is:

$$t_R = \frac{1}{am\sigma_o^m}\left[1-\left[1-\sigma_o^{m-k}\frac{a(m-k)}{b(k+1)}\right]^{m/(m-k)}\right] \quad \ldots \quad (2.16)$$

which is shown by line m in fig. (2.10). The time t':

$$t' = \frac{1}{am}\left[\frac{b(k+1)}{a(m-k)}\right]^{-m/(m-k)}$$

in fig. (2.10) indicates whether mixed Kachanov or ductile theories apply.

2.4.4 Robinsons life fraction rule

A different view of damage was proposed by Robinson. The component deteriorates in proportion to the ratio of time spent at a particular load and temperature to the rupture time at that load and temperature [1], i.e. the deterioration accumulated during t_i at s_i and T_i, is:

$$d_i = t_i/t_{Ri}$$

The damage from each load case i is independent of any previous loading, but accumulates with damage from previous loads. For step loading, rupture is taken to occur when [5]:

$$d_f = \sum_i t_i/t_{Ri} = 1.0$$

Or for continuously varying loads, rupture occurs when:

$$\int \frac{dt}{t_R} = 1.0$$

In practice, rupture was found to occur at cumulative damage values significantly different from 1.0, ranging between 0.4 and 2.0 depending on the load sequence. It was shown [17] that the cumulative life fraction at failure is less than 1.0 when stresses increase with time, and greater than 1.0 for stresses decreasing with time.

Also the life fraction rule makes no distinction between damage accrued under stress and temperature. Creep-damage behaviour under changing stresses is, however, fundamentally different from creep damage behaviour under changing temperature.

Despite these misgivings, the life-fraction rule yields acceptable results, considering scatter in rupture data. It is simple to apply using readily availible data. In [17] lines of constant damage were correlated with the Larson-Miller parameter, indicating that the life fraction rule is also

consistent for temperature changes. Although it is inaccurate for load changes, it could still be applied successfully if tests could indicate what cumulative damage fraction other than 1.0 applies to the load sequence in question.

Although Kachanov defines damage differently, it can be shown [1] that the Kachanov approach under variable loads reduces to the life fraction rule, indicating that the theories are consistent with one another.

2.5 Integration of the constitutive model

Of the various creep and damage evolution theories discussed in sections 2.3 and 2.4, the creep equation (2.9) and damage equation (2.13) will be chosen for further development. The complete material constitutive model thus is:

$$\dot{\lambda}_{crij} = \frac{3}{2} \frac{\Sigma_{eN}^{m-1} D_{ijN}}{(1-\omega)^m} \qquad \ldots \quad (2.9)$$

and

$$\dot{\omega} = \frac{b\sigma_o^{k+1-m}}{aE} \frac{\left[\alpha\Sigma_{1N} + (1-\alpha)\Sigma_{eN}\right]^k}{(1-\omega)^p} \qquad \ldots \quad (2.13)$$

Because the stresses continually vary in time, the constitutive equations must be integrated numerically. The time increment $\Delta\tau$ is chosen sufficiently small so that constant stresses can be assumed during that time step. The damage evolution equation can be integrated analytically within the time step ${}_n\tau < \tau < {}_{n+1}\tau$ to obtain the damage at the end of the step n:

$${}_{n+1}\omega = 1 - \left[(1-{}_n\omega)^{p+1} - \Delta\tau/\tau_R\right]^{1/(p+1)} \qquad \ldots \quad (2.17)$$

with:

$$\tau_R = \frac{1}{C(p+1)\left[\alpha\Sigma_{1N} + (1-\alpha)\Sigma_{eN}\right]^k} \qquad \ldots \quad (2.18)$$

This τ_R does not provide an indication of the time to failure of the component, as the stresses are not constant. If the nominal stresses were to remain constant, as in the uniaxial case, then τ_R would indicate the component lifetime. Noting that:

$$[1-\omega(t)]^m = [(1-{}_n\omega)^{p+1} - (\tau-{}_n\tau)/\tau_R]^{m/(p+1)} \qquad {}_n\tau<\tau<{}_{n+1}\tau$$

the creep evolution equation can be analytically integrated over the time step, so that the creep strain increment during the timestep n is:

$$\Delta\lambda_{crij} = \frac{3\Sigma_{Ne}^{m-1} D_{Nij}}{2C(p+1-m)\left[\alpha\Sigma_{N1}+(1-\alpha)\Sigma_{Ne}\right]^k}\left[(1-{}_n\omega)^{p+1-m} - (1-{}_{n+1}\omega)^{p+1-m}\right]$$

The creep strain at the end of the time step is:

$${}_{n+1}\lambda_{crij} = {}_n\lambda_{crij} + \Delta\lambda_{crij} \qquad \ldots \quad (2.19)$$

This forward-difference algorithim can now be used by noting that at $\tau=0$, $\omega=0$ $\lambda_{cr}=0$ and the stresses are obtained from the elastic solution. At each subsequent time step $n=1,2 \ldots n_R$, τ_R and thus ${}_{n+1}\omega$ and ${}_{n+1}\lambda_{cr}$ can be found. The equilibrium and continuity equations applied at the end of every time increment will yield the changes in the stress pattern. Whenever $\omega \approx 1$, rupture has occurred, and the damage and creep accumulation must cease.

If the refined damage model is used, damage is suppressed in compression. Then equations (2.17) and (2.18) are modified, whenever the maximum principal stress is compressive, to:

$$\omega = 0 \qquad \Sigma_1 < 0 \qquad \ldots \quad (2.17a)$$

$$\tau_R = \infty \qquad \Sigma_1 < 0 \qquad \ldots \quad (2.18a)$$

The integration of equation (2.9a) yields in compression:

$$^{n+1}\lambda_{crij} = {}^{n}\lambda_{crij} + 3/2\Sigma_{Ne}{}^{m-1}S_{Nij}\,\Delta\tau \qquad \Sigma_1 < 0 \quad \ldots \quad (2.19a)$$

A simple forward-difference algorithim is acceptable as the time step is chosen such that the stress can be considered constant over the interval. Also, equation (2.19) was derived using a forward-difference algorithim of comparable accuracy.

3.0 Creep predictions for bending beams

3.1 Primary creep and stress redistribution in a beam subject to bending and axial loads

Upon loading virgin material, an initially very high strain rate is observed, which progressively decreases to a constant creep strain rate referred to as the steady state. Secondary creep is then seen as a continuation of this steady state [1].
The primary creep phenomenon can be explained to be a result of an interaction between creep and elastic strains caused by a redistribution of stress.

When a component is loaded, the stress distribution is initially elastic. However, since the creep strain rate is a nonlinear function of stress, the stresses must redistribute so as to maintain equilibrium and continuity at all times. At the steady state the redistribution is complete (to a sufficiently high degree) and the stresses remain constant thereafter.
The analysis for a beam in bending and axial load follows to illustrate the method used to predict primary creep. In principle the same method is used to predict primary creep in any geometry.

For every case the analysis method comprises the following procedure [1]:

1) Solve the elastic problem subject to its boundary conditions for stresses and strains, i.e. solve the relevant governing differential equations at t=0.

2) Choose a constitutive relationship to describe creep behaviour. Usually a power function of stress is sufficient.

3) Noting that subsequent (t>0) strain comprises the sum of elastic and creep strains, obtain the rate form of the governing differential equations. This will include additional terms incorporating creep strain.

4) Solve the rate equations subject to the boundary conditions, bearing in mind that the complete solution at each time step comprises a particular integral (obtained in 1 above) and a complementary function. Expressions for strain rate, stress rate and creep rate (as appropriate) are obtained. These are integrated numerically (forward difference is amenable and sufficient) to obtain all quantities at the following time step. Equilibrium must be enforced to obtain the complete solution at that time step..

5) Step 4) is repeated from time step to time step using the most current infomation until a steady-state is reached. Criteria for the attainment of the steady-state would be either a sufficiently constant strain rate or a sufficiently small stress rate.

In practice this method becomes very complicated for more realistic geometries, and a finite element method would be more appropriate. However in principle the method is still applicable [1].

The analysis neglects strains other than elastic and creep strains, as well as damage accumulation, but does include the possibility of step loads.

3.1.1 Time hardening

Consider a beam-element in tension and bending [11]:

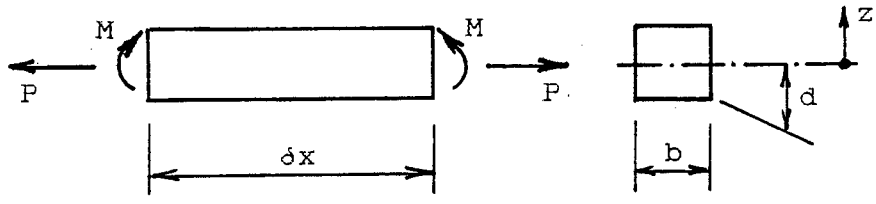

The strain comprises the sum of the elastic and creep strains, or alternatively, the sum of the strains due to bending and tension. Continuity requires [1]:

$$\epsilon_x = \frac{\sigma_x}{E} + \epsilon_{cr} = \kappa z + \epsilon_x(0) \qquad \ldots \quad (3.1)$$

Solving for stress:

$$\sigma_x = E\left[\epsilon_x(0) + \kappa z - \epsilon_{cr}\right] \qquad \ldots \quad (3.2)$$

Force and moment equilibrium require:

$$P = \int_A \sigma_x \, dA \qquad \text{and} \qquad M = \int_A \sigma_x \, z \, dA$$

which after partial integration yield:

$$P = EA\epsilon_x(0) - E\int_A \epsilon_{cr} \, dA$$

$$M = EI\kappa - E\int_A \epsilon_{cr} \, z \, dA \qquad \ldots \quad (3.3)$$

If creep strain is zero, the above reduces to the familiar elastic case.

Non-dimensionalising, using:

$$\Sigma = \sigma/\sigma_o \qquad \lambda = \epsilon/\epsilon_o \qquad \xi = z/d$$

$$\alpha = d^2/A \qquad \beta = d^4/I$$

where σ_o is the reference stress, equations (3.1), (3.2) and (3.3) become:

$$\lambda_x = \Sigma_x + \lambda_{cr} = \lambda_o + \frac{\kappa d}{\epsilon_o}\xi \qquad \ldots \quad (3.1a)$$

$$\Sigma_x = \lambda_{xo} + \frac{\kappa d}{\epsilon_o}\xi - \lambda_{cr} \qquad \ldots \quad (3.2a)$$

$$\frac{P}{\sigma_o} = \frac{d^2\,\lambda_{xo}}{\alpha} - \int_{-1}^{+1} \lambda_{cr}\, d^2\eta\, d\xi$$

$$\frac{M}{\sigma_o} = \frac{d^4\,\kappa}{\beta\,\epsilon_o} - \int_{-1}^{+1} \lambda_{cr}\, d^3\eta\xi\, d\xi \qquad \ldots \quad (3.3a)$$

A non-dimensional time-parameter is used, and is defined as:

$$\tau = \int E\sigma_o^{m-1}\, f_2(t)\, dt$$

and all the following time derivatives ($\dot{}$) are with respect to this τ. This is convenient as the analysis is now independent of f_2, and f_2 only affects the transformation from the τ domain to real time.

Using f_1 from section 2.1 the time hardening creep law is:

$$\dot{\lambda}_{cr} = \Sigma_x^m \qquad \ldots \quad (3.4)$$

At τ=0: the elastic solution is found by noting that τ=0.

$$\lambda_x = \Sigma_x \qquad \ldots \quad (3.1b)$$

$$S_x = \frac{P}{A\sigma_o} + \frac{Md}{I\sigma_o}\xi \qquad \ldots \quad (3.2b)$$

$$\lambda_{xo} = \frac{P}{A\sigma_o}$$

$$\ldots \quad (3.3b)$$

$$\frac{\kappa}{\epsilon_o} = \frac{M}{I\sigma_o}$$

At τ>0: the rate equations are obtained by differentiating equations (3.1a), (3.2a) and (3.3a) with respect to τ, and substituting from (3.4):

$$\dot{\lambda}_x = \dot{\Sigma}_x + \dot{\Sigma}_x^m \qquad \ldots \quad (3.1c)$$

$$\dot{\Sigma}_x = \frac{\dot{P}}{A\sigma_o} + \frac{\dot{M}d}{I\sigma_o}\xi + \alpha\int_{-1}^{+1}\Sigma_x^{m_\eta}\,\partial\xi + \beta\xi\int_{-1}^{+1}\Sigma_x^{m_{\eta\xi}}\,\partial\xi - \Sigma_x^m \qquad \ldots \quad (3.2c)$$

taking $\dot{P}$ and $\dot{M}$ =0:

$$\dot{\lambda}_{xo} = \alpha\int_{-1}^{+1}\Sigma_x^{m_\eta}\,d\xi \qquad \ldots \quad (3.3c)$$

$$\frac{\dot{\kappa}}{\epsilon_o} = \frac{\beta}{d}\int_{-1}^{+1}\Sigma_x^{m_{\eta\xi}}\,d\xi$$

Two approaches can be used in the algorithim:

First Approach:
Numerically integrate [1] $\dot{\Sigma}_x$, $\dot{\lambda}_{xo}$, $(\dot{\kappa}/\epsilon_o)$ thus:

$$\Sigma_x^{j+1} = \Sigma_x^j + \dot{\Sigma}_x^j\,\Delta t \qquad \text{and} \qquad \lambda_{xo}^{j+1} = \lambda_{xo}^j + \dot{\lambda}_{xo}^j\,\Delta t$$

$$\text{and} \qquad (\kappa/\epsilon_o)^{j+1} = (\kappa/\epsilon_o)_j + (\dot{\kappa}/\epsilon_o)^j\,\Delta\tau$$

$$\text{so:} \qquad \lambda_{cr}^{j+1} = \Sigma_x^{j+1} - \lambda_{xo}^{j+1} - (\kappa/\epsilon_o)^{j+1}d\xi$$

$$\text{and:} \qquad \lambda_x^{j+1} = \lambda_{xo}^{j+1} + (\kappa/\epsilon_o)^{j+1}d\xi$$

and check errors made by using equation (3.3a) at regular intervals.

Second Approach:
Numerically integrate [12] $\dot{\lambda}_{cr}$ only.

$$\lambda_{cr}^{j+1} = \lambda_{cr}^j + \dot{\lambda}_{cr}^j\Delta\tau$$

and obtain λ_{xo} and (κ/ϵ_o) from eq. (3.3a), λ_x from eq. (3.1a), and Σ_x from (3.2a). A refinement is possible when instead of using Σ_x at the beginning of the interval, the average Σ on that interval is chosen:

$$\lambda_{cr}^{j+1} = \lambda_{cr}^j + \left[\Sigma_x^j + 1/2\dot{\Sigma}_x^j\Delta\tau\right]^m\Delta\tau$$

Check errors by comparing results from equation (3.2a) with:

$$\Sigma_x^{j+1} = \Sigma_x^j + \dot{\Sigma}_x^j\Delta t$$

3.1.2 Strain hardening

The analysis is exactly the same as for time hardening [12] up to the point where a creep law is used in equation (3.4). From there:

Using f_1 from section 2.1 the strain hardening law is:

$$\dot{\lambda}_{cr} = \frac{nA^{1/n}\sigma_o^{(m-1)/n}\Sigma_x^{m/n}}{\lambda_{cr}^{(1-n)/n}} \qquad \ldots \quad (3.5)$$

For $\tau=0$: the elastic solution is as before.

For $\tau>0$: the rate equations are:

$$\dot{\lambda}_x = \dot{\Sigma}_x + \dot{\lambda}_{cr} \qquad \ldots \quad (3.1d)$$

$$\dot{\Sigma}_x = \dot{\lambda}_{xo} + (\kappa/\epsilon_o)\dot{d\xi} - \dot{\lambda}_{cr} \qquad \ldots \quad (3.2d)$$

for $\dot{P}$ and $\dot{M} = 0$:

$$\dot{\lambda}_{xo} = \alpha\eta\int_{-1}^{+1}\dot{\lambda}_{cr}\,d\xi \quad , \quad (\kappa/\epsilon_o)^{\cdot} = \beta\eta/d\int_{-1}^{+1}\dot{\lambda}_{cr}\,\xi\,d\xi \qquad \ldots \quad (3.3d)$$

The two approaches that can now be followed are the same as for the time hardening case exept that now the equation set (*.*d) must be used.

A subsequent step change in load can be dealt with in exactly the same way as a constant load applied to virgin material, exept that now the material has initial stresses, strains and deflections.

The results of time hardening and strain hardening primary creep, and the stress redistribution are illustrated in fig. (3.1):

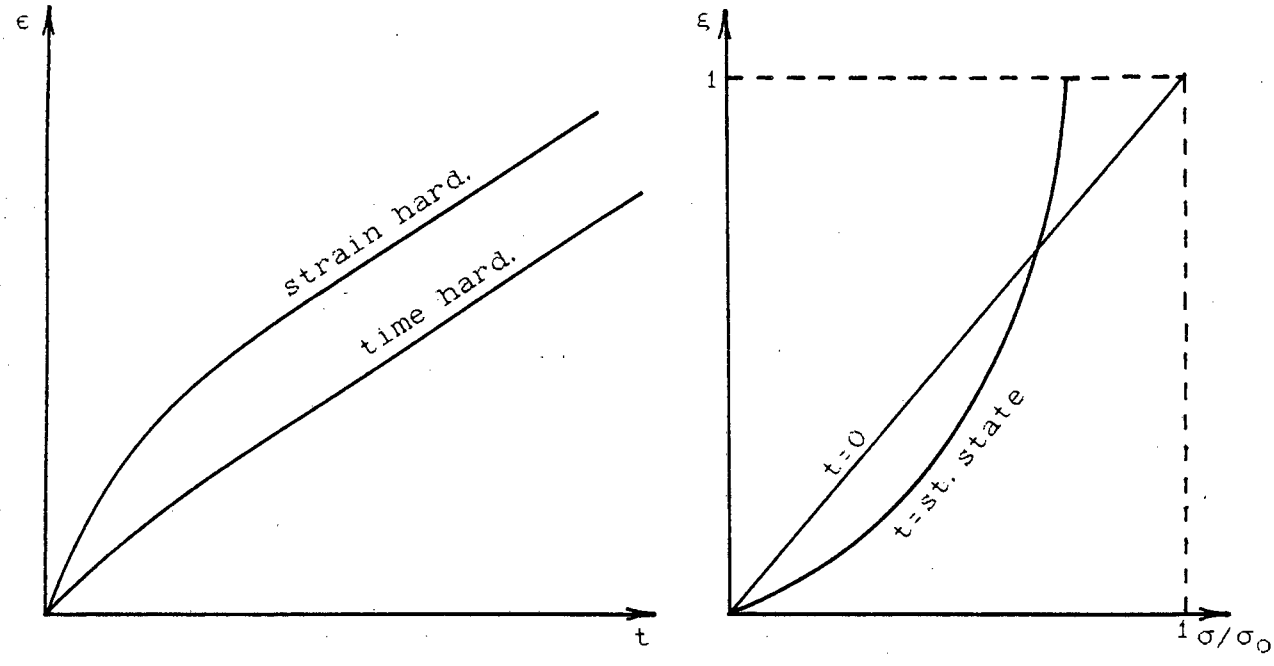

fig. (3.1) Primary creep - time and strain hardening

For the special case of a beam subject to an axial load only, no stress redistribution takes place. For loads other than step loads, equations (3.3c) or (3.3d) will have to be re-evaluated to incorporate additional load rate terms.

3.2 Creep predictions for a beam subject to damage

In order to predict the complete creep response of a beam to steady axial and bending loads, a constitutive relationship must be found that models the tertiary phase of creep. Kachanov's notion of damage [4], defined as a progressive reduction of the load-bearing area, appears to reproduce the trends observed during tertiary creep rather well. This damage equation must be combined with the algorithims describing stress redistribution (section 3.1), as damage accumulation rates have been shown to be strongly dependent on stress.

The Kachanov brittle damage theory will be used, although this theory is limited to the lower stress region, as shown in section 2.4.1. This is not considered to be too restrictive, as in most design situations only the long life, low stress regions are of interest.

Further, the refinement of the Kachanov damage theory will be used, whereby an attempt is made to model crack closure under compression. It has been argued [18] that under compression any cracks close, and so the undamaged area is available to bear load, whereas in tension the load bearing area is progressively reduced by damage. Further, it is claimed that microcracks do not grow under compressive stress. This is equivalent to saying that the creep rupture life in compression is infinity, and that no tertiary phase exists in compression. This is clearly not true, as graphs of compressive creep display the same tertiary characteristics as their tensile counterparts [19]. The graphs in [19] seem to indicate that the rupture life in compression is about an order of magnitude higher than the rupture life in tension for the similar loads. So damage rates are significantly lower in compression than in tension, and a component will have ruptured in a region of tensile stress long before any appreciable damage could accumulate in the regions of compressive stress. On the other hand, for other materials, noticeably copper, no differences between tensile and compressive damage rates were observed [22]. So to disallow damage in compression is valid for specific materials only. To set damage in compression equal to zero appears to be acceptable whenever there are tensile loads that dominate damage accumulation and rupture. Should the entire component be under compressive loads however, it would be invalid to assume no damage accumulation in compression. The damage accumulation rate in compression would be significantly lower than the rate in tension.

It has repeatedly been observed that microcracks in tension preferentially grow on planes perpendicular to the maximum principal stress (i.e. an opening mode I crack). It has been shown [22] that under compression damage accumulates on a different plane, namely the plane of maximum principal shear stress (i.e. a sliding mode II or tearing mode III type crack).

Questions now arise in how to calculate the accumulation of damage that is generated on different planes. Tests conducted on tubes in tension and reverse torsion indicate that damage accumulated on different planes do not interact. Tensorial representations of damage [30] have been formulated in order to

capture not only the amount, but also the orientation of damage. Hayhurst [20] used principal damage rates in three principal stress directions with some success.

The damage equations that will be used here are:

$$\frac{\partial \omega}{\partial t} = b\sigma^{k} \qquad \sigma > 0$$

$$\omega \,, \quad \frac{\partial \omega}{\partial t} = 0 \qquad \sigma \leq 0$$

Concerning this non-linear Kachanov constitutive relationship, a further point can been raised [18]. Should loads change between tension and compression, damage will be a discontinuous function: Damage is accumulated under tension, and as the loads become compressive damage "jumps" to zero. Clearly, finite damage exists, although during compressive loads damage is not incorporated into the equations, thus simulating crack closure. During the compressive phase, the material "remembers" the damage accumulated in tension. Upon resumption of the tensile load, damage "jumps" back to its original value and continues to accumulate.

A further complication arises out of the non-linear damage equation, in that equilibrium can only be maintained if the stresses redistribute during damage accumulation. So stresses change not only during primary creep, but during tertiary creep also, and the notion of a steady-state stress distribution no longer exists.

It has been shown [21] that in bending the neutral axis shifts away from the region of high damage. Stresses redistribute in such a way so as to relieve highly damaged areas from bearing load, but at the expense of higher stresses in lesser damaged areas.

The analysis that follows is an enlargement on the theory presented in section 3.1.1. and incorporates non-linear damage accumulation. The time-hardening assumption has been retained although it is conceded that the response to varying loads will be poorly modelled. In principle any beam cross section can be considered, however only rectangular and circular cross sections will be elaborated on in the appendix A.

Consider a beam under tension and/or bending:

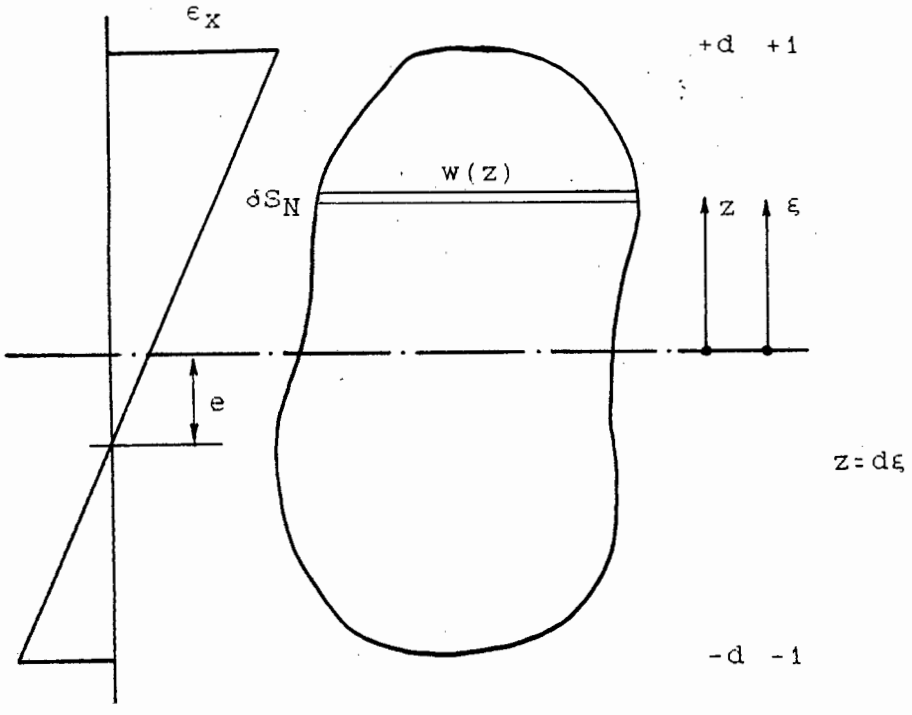

fig. (3.2) Beam section

As plane sections remain plane,

$$\epsilon_x = \epsilon_x(z=0) + \kappa z = E^{-1}\sigma_x + \epsilon_{cr} \qquad \ldots \quad (3.1)$$

$$\sigma_x = E[\epsilon(0) + \kappa z - \epsilon_{cr}] \qquad \ldots \quad (3.2)$$

Non dimensionalising:

$$\lambda_x = \lambda_{x0} + (\kappa/\epsilon_0)*d\xi = \Sigma_x + \lambda_{cr} \qquad \ldots \quad (3.1e)$$

$$\Sigma_x = \lambda_{x0} + (\kappa/\epsilon_0)*d\xi - \lambda_{cr} \qquad \ldots \quad (3.2e)$$

At the neutral axis $\epsilon(e)=0$, so:

$$e = -\epsilon(0)/\kappa$$

Equilibrium must consider the actual stress σ_x acting on the load bearing area (dS), which is reduced by damage:

$$P = \int_S \sigma_x \, dS \qquad\qquad M = \int_S \sigma_x z \, dS$$

As the limits of integration vary with damage, the current load bearing area dS is related to the original, undamaged area dS_N by:

$$dS = (1-\omega)\, dS_N$$

so that:

$$P=\int_{S_N} \sigma_x(1-\omega)\ dS_N \qquad M=\int_{S_N} \sigma_x(1-\omega)z\ dS_N \qquad \ldots \quad (3.3)$$

Or in non-dimensional form:

$$\frac{P}{\sigma_0}=\int_{S_N} \Sigma_x(1-\omega)\ dS_N \qquad \frac{M}{\sigma_0}=\int_{S_N} \Sigma_x(1-\omega)z\ dS_N \qquad \ldots \quad (3.3e)$$

Substituting from equation (3.2e):

$$\begin{bmatrix} I_1 & I_2 \\ I_2 & I_3 \end{bmatrix} \begin{bmatrix} \lambda_{x0} \\ \dfrac{\kappa}{\epsilon_0} \end{bmatrix} = \begin{bmatrix} \dfrac{P}{\sigma_0} + I_4 \\ \dfrac{M}{\sigma_0} + I_5 \end{bmatrix}$$

where:

$$I_1=\int_{S_N}(1-\omega)\ dS_N \qquad I_2=\int_{S_N}(1-\omega)d\xi\ dS_N \qquad I_3=\int_{S_N}(1-\omega)d^2\xi^2\ dS_N$$

$$I_4=\int_{S_N}\lambda_{cr}(1-\omega)\ dS_N \qquad I_5=\int_{S_N}\lambda_{cr}(1-\omega)d\xi\ dS_N$$

In appendix A the integrals are given for both rectangular and circular beam cross sections. So:

$$\begin{bmatrix} \lambda_{x0} \\ \dfrac{\kappa}{\epsilon_0} \end{bmatrix} = \frac{1}{I_1 I_3 - I_2^2} \begin{bmatrix} I_3 & -I_2 \\ -I_2 & I_1 \end{bmatrix} \begin{bmatrix} \dfrac{P}{\sigma_0} + I_4 \\ \dfrac{M}{\sigma_0} + I_5 \end{bmatrix} \qquad \ldots \quad (3.6)$$

Given loads and creep strains at any time, the equilibrium stress distribution can be obtained from equations (3.6) and (3.2e) after evaluating the integrals I_1 to I_5.

The equilibrium-rate equations are from equation (3.3e):

$$\frac{\dot{P}}{\sigma_0} = \int_{S_N} \dot{\Sigma}_x (1-\omega)\ dS_N - \int_{S_N} \Sigma_x \dot{\omega}\ dS_N$$

$$\frac{\dot{M}}{\sigma_0} = \int_{S_N} \dot{\Sigma}_x (1-\omega)\, d\xi\ dS_N - \int_{S_N} \Sigma_x \dot{\omega}\, d\xi\ dS_N$$

where the first and second terms in either equation describe stress redistribution during primary and tertiary creep respectively.

From equation (3.2e):

$$\dot{\Sigma}_x = \dot{\lambda}_{x0} + (\dot{\kappa}/\epsilon_0)\, d\xi - \dot{\lambda}_{cr} \qquad \ldots \quad (3.7)$$

and proceding similarly as before:

$$\begin{bmatrix} \dot{\lambda}_{x0} \\ \dot{\kappa}/\epsilon_0 \end{bmatrix} = \frac{1}{I_1 I_3 - I_2^2} \begin{bmatrix} I_3 & -I_2 \\ -I_2 & I_1 \end{bmatrix} \begin{bmatrix} \dot{P}/\sigma_0 + I_6 + I_8 \\ \dot{M}/\sigma_0 + I_7 + I_9 \end{bmatrix} \qquad \ldots \quad (3.8)$$

with:

$$I_6 = \int_{S_N} \dot{\lambda}_{cr} (1-\omega)\ dS_N \qquad I_7 = \int_{S_N} \dot{\lambda}_{cr} (1-\omega)\, d\xi\ dS_N$$

$$I_8 = \int_{S_N} \Sigma_x \dot{\omega}\ dS_N \qquad I_9 = \int_{S_N} \Sigma_x \dot{\omega}\, d\xi\ dS_N$$

Also see appendix A.

By substituting equation (3.8) back into equation (3.7), the stress rate at any time is known. This enables a time step to be chosen: Integrating the constitutive equations presupposes a constant - or rather an acceptably constant - stress during a time step $\Delta\tau$. If a 1% variation in stress is considered acceptable,

$$\Sigma_{x\ j} + \dot{\Sigma}_{x\ j} \Delta\tau = \Sigma_{x\ j+1} = 1.01 \Sigma_{x\ j}$$

As Σ_x and $\dot{\Sigma}_x$ vary throughout the cross section, the smallest quotient is selected:

$$\Delta\tau = 0.01 \left| \frac{\Sigma_x}{\dot{\Sigma}_x} \right| \text{ smallest} \qquad \ldots (3.9)$$

as proposed in [1].

So far the analysis has been general, and at this point the non linear Kachanov constitutive equation can be introduced.

Creep	Damage	
$\epsilon_{cr}=f_1(\sigma)\ f_2(t)\ f_3(T)$	$\omega=F_1(\sigma)\ f_2(t)\ f_3(T)$	$\sigma_N>0$
	$=0$	$\sigma_N\leq 0$

For constant temperature, using the Norton and Bailey relationships:

$\epsilon_{cr}=a\sigma^m\ t^n$	$\omega=b\sigma^k\ t^n$	$\sigma_N>0$
	$=0$	$\sigma N\leq 0$

with

$$\sigma_x = \frac{\sigma_{xN}}{(1-\omega)} \qquad \sigma_N>0$$

$$=\sigma_{xN} \qquad \sigma_N\leq 0$$

Non-dimensionalising the above using the non dimensional time parameter τ:

$$\tau=At^n \quad \text{with} \quad A=aE\sigma_0^{m-1} \quad \text{and} \quad B=\frac{b\sigma_0^{k+1-m}}{aE}$$

yields:

$$\dot{\lambda}_{cr} = \left[\frac{\Sigma_{xN}}{1-\omega}\right]^m \qquad \Sigma_{xN}>0$$

$$= \Sigma_{xN}^m \qquad \Sigma_{xN}\leq 0 \qquad \ldots (3.10)$$

and

$$\dot{\omega} = B\left[\frac{\Sigma_{xN}}{1-\omega}\right]^k \qquad \Sigma_{xN}>0$$

$$\omega\ ,\ \dot{\omega} = 0 \qquad \Sigma_{xN}\leq 0 \qquad \ldots (3.11)$$

The analysis that follows is taken from [15] and has been reproduced in section 2.4.1 for the case of steady state creep. Here, stress redistribution due to damage is included.

Integrating equation (3.11) yields:

$$\tau_R = \frac{1}{B(k+1)\Sigma_{xN}^{k}} \qquad \Sigma_{xN}>0$$

$$= \infty \qquad \Sigma_{xN}\leq 0 \qquad \ldots (3.12)$$

and transforming back to the real time domain:

$$t_R^{n} = \frac{1}{b(k+1)\sigma_{xN}^{k}} \qquad \sigma_{xN}>0$$

$$= \infty \qquad \sigma_{xN}\leq 0 \qquad \ldots (3.12a)$$

Given sufficiently constant stresses over the time interval $\Delta\tau$ (a 1% variation is considered acceptable), the damage increment between τ_i and $\tau_i+\Delta\tau_i$ is:

$$\omega_{i+1} = 1-\left[(1-\omega_i)^{k+1} - \frac{\Delta\tau}{\tau_R}\right]^{(1/(k+1))} \qquad \Sigma_{xN}>0$$

$$= \omega_i \qquad \Sigma_{xN}\leq 0 \qquad \ldots (3.13)$$

Integrating equation (3.10) over $\Delta\tau$ yields the creep strain increment :

$$\Delta\lambda_{cri} = \frac{\Sigma_{xN}^{m-k}}{B(k+1-m)}\left[(1-\omega_i)^{k+1-m} - (1-\omega_{i+1})^{k+1-m}\right] \qquad \Sigma_{xN}>0$$

$$= \Sigma_{xN}^{m}\,\Delta\tau \qquad \Sigma_{xN}\leq 0 \qquad \ldots (3.14)$$

so:

$$\lambda_{cr\ i+1} = \lambda_{cr\ i} + \Delta\lambda_{cri}$$

Transforming back to the real time domain:

$$\epsilon_{crR} = \frac{a\sigma^{m-k}}{b(k+1-m)} \qquad \sigma_{xN}>0$$

$$= \infty \qquad \sigma_{xN}\leq 0 \qquad \ldots (3.14a)$$

Also:

$$\lambda_{crR} = \dot{\lambda}_{cr\ min}\, L\, \tau_R \quad \text{where} \quad L = \frac{k+1}{k+1-m} \text{ the creep ductility.}$$

Now the constants a and b and the exponents m, n, K must be found. This ammounts to curvefitting selected equations against experimental data. For this purpose data from [19] for the alloy Mar-M 246 at 900 C has been chosen. It must be noted from the outset that finding equation constants that yield acceptable results is no easy matter, in view of the extreme sensitivity of the predicted creep response to even the slightest variations in an equation constant.